

MAP estimation for Multiresolution Fusion in Remotely Sensed Images using an IGMRF Prior Model

Manjunath Joshi, Member IEEE, and André Jalobeanu, Member IEEE

Abstract— In this paper we propose a model based approach for the multiresolution fusion of satellite images. Given the high spatial resolution panchromatic (Pan) image and a low spatial and high spectral resolution multispectral (MS) image acquired over the same geographical area the problem is to generate a high spatial and high spectral resolution multispectral image. This is clearly an ill-posed problem and hence we need a proper regularization. We model each of the low spatial resolution MS images as the aliased and noisy versions of their corresponding high spatial resolution i.e., fused (to be estimated) MS images. A proper aliasing matrix is assumed to take care of the undersampling process. The high spatial resolution MS images to be estimated are then modeled as separate Inhomogeneous Gaussian Markov Random Fields (IGMRF) and a *Maximum A Posteriori* (MAP) estimation is used to obtain the fused image for each of the MS bands. The IGMRF parameters are estimated from the available high resolution Pan image and are used in the prior model for regularization purposes. Since the method does not directly operate on the Pan pixel values as most of the other methods do, the spectral distortion is minimum and the spatial properties are better preserved in the fused image as the IGMRF parameters are learned at every pixel. We demonstrate the effectiveness of our approach over some existing methods by conducting the experiments on synthetic data as well as on the images captured by the Quickbird satellite.

Index Terms - Inhomogeneous Gaussian markov random field, decimation, multiresolution fusion, super-resolution, multispectral image, panchromatic image.

I. Introduction

It is very difficult to provide an accurate definition for image fusion. In general terms, it is an approach to information extraction by combining the non redundant information available in several images. Considering the lack of appropriate definition, a European working group formed in the year 1996 gave the following definition for data fusion [1]. *Data fusion is a formal framework in which are expressed the means and tools for the alliance of data originating from different sources.* In remote sensing, the availability of large numbers of images of the land mass taken at different spatial and spectral resolutions at different times using multiple sensors has made the research on fusion very meaningful. In many applications it is very much beneficial to have high spatial and spectral resolution images. On one hand the high spatial resolution is necessary for accurate description of the features and structures and on the other hand different objects are better identified if a high spectral resolution is used. Multiresolution fusion is a process of combining a high spatial resolution panchromatic image (Pan) and a low spatial but high spectral resolution multispectral (MS) image to produce a high spatial and spectral resolution MS image. Due to the physical constraints on the satellite sensor, the multispectral images are generally captured with lower spatial resolution than the Pan image. Since the information obtained from individual sensors is often incomplete, inconsistent, or imprecise [2], [3], the image produced by fusing the information from different sensors results in better understanding of the acquired data that helps for a better analysis of the scene segments.

The area of multiresolution fusion is quite matured with many researchers attempting to solve this problem for remote sensing applications. The most common method is the intensity-hue-

saturation transform (IHST) technique [4], [5], [6], [7]. This technique can enhance the spatial details, but also produces spectral distortion. The fusion approach based on the high pass filtering (HPF) [8], [9] technique injects the high spatial frequency details from the pan image into the up sampled versions of MS images. Although these methods have demonstrated better performance, improving the quality of spatial details and thus showing a better visual effect, they also amplify the noise. Other approaches considered for multiresolution fusion in the remote sensing literature include principal component transform (PCT) [10], [11] and wavelet transform (WT) based approaches [12], [13], [14], [15]. The standard WT method is based on replacing the high frequency component of the MS images with that of Pan image by working in the wavelet domain and then synthesizing the fused image by applying the inverse wavelet transform. Fusion schemes based on the "à trous" wavelet (ATW) algorithm have been also proposed [16], [17], [18]. In [19], Aiazzi et al. propose two context driven fusion methodologies based on an undecimated discrete wavelet transform (UDWT) and a generalized Laplacian pyramid (GLP), respectively. The former uses an octave bandpass representation obtained from a conventional wavelet transform by omitting the decimators and upsampling the wavelet filter bank: the latter is based on another oversampled structure obtained by recursively subtracting from an image an expanded and decimated low pass version. In one of the recent works on multiresolution fusion[20], the authors use the curvelet transforms for enhancing the MS bands. They inject the high frequency directional components into the MS bands after extracting them using the curvelet transform on the Pan image. Authors in [21] improve the performance of IHST and PCA mergers using wavelet decomposition. Ranchin et al., [22] propose some successful implementation schemes for fusion using ARSIS (spatial resolution enhancement by injection of structures) concept. The other research works in fusion include [23], [24], [25], [26], [27], [28], [29], [30], [31]. More recent works can be found in [32], [33], [34], [35], [36], [37], [38], [39], [40], [41].

All the above methods require accurate coregistration before the fusion process takes place. The upsampling of the MS image using a standard interpolation technique before the fusion process does not consider the aliasing present in the low resolution observation and causes the fused images to suffer from the problem of aliasing and hence introduces distortion in the fused image. Also when fusing the Pan and MS images acquired by different satellites the pixel values of the Pan data may differ significantly from the MS images due to the change in sensor, but the spatial correlation does not get affected since the images are acquired over the same region. This may be a practical constraint affecting the fusion results while solving the fusion problem that operate directly on Pan pixel values.

In this paper we solve the multiresolution fusion problem

based on a different concept called *super-resolution*. Super-resolution refers to a signal processing approach for obtaining a high spatial resolution image from images that are captured using a low spatial resolution sensor by combining the non-redundant data available in the aliased low resolution observations. Many of the researchers have attempted to solve the super-resolution problem by using the motion cue, where a number of low resolution observation are captured with subpixel shifts to obtain a single high resolution image. In recent years researchers in the field of image processing have used learning based methods for super-resolution where the high resolution properties are learned using a part of the available high resolution image [42] or from a set of training images [43], [44]. Our work in this paper is based on the model based approach proposed in [45]. Here the authors proposed an autoregressive (AR) model based multiresolution fusion technique for fusing the Pan and MS images. The approach is based on learning the homogeneous AR parameters (24 parameters estimated over the entire image) from the available Pan image and using these parameters in a prior model for regularization. The low resolution MS image is modeled as the aliased version of the corresponding high resolution image and a suitable regularization is used to obtain the high resolution MS image. A fixed decimation matrix is used to represent the aliasing present in the low spatial resolution MS images. Although the method can be employed for images that are not accurately registered, the method has the following drawbacks:

1. Few homogeneous AR parameters learned globally from Pan image using a fixed neighborhood fail to capture the spatial dependency among pixels very well as satellite images contain significant texture with well localized features and it is more appropriate to use an inhomogeneous prior for describing these.
2. In general the AR model is more effective on moderately high resolution images rather than on very high resolution images, since the finer details are not captured well by the AR process.

The work described in this paper is based on our earlier work published in [46]. In this paper we use an MRF-based modeling for capturing the spatial correlation among pixels in the high resolution MS image. It is well known that MRFs are the most general models used as a priors during regularization when solving ill-posed problems. In order to preserve discontinuities as well as reconstruct the smooth areas well, we use an inhomogeneous GMRF as a prior model instead of an AR model. This enables us to capture the smooth regions as well as the sudden intensity variation due to sharp edges. We estimate these inhomogeneous parameters from the available high resolution Pan image as both the MS and Pan images cover the same geographical area. In particular, we estimate four GMRF parameters at every location of the Pan image. Our fusion process is less influenced by the spectral properties of the high spatial resolution Pan image used for learning when compared to other methods. This enhances the spatial information of the fused MS images while keeping the spectral properties intact.

It is of interest to note that the researchers in [47] also propose a model based approach for fusion. They use an image formation model based on the spectral consistency which is based on the received light intensity and the frequency response for a particular channel. Different regularization schemes are used to

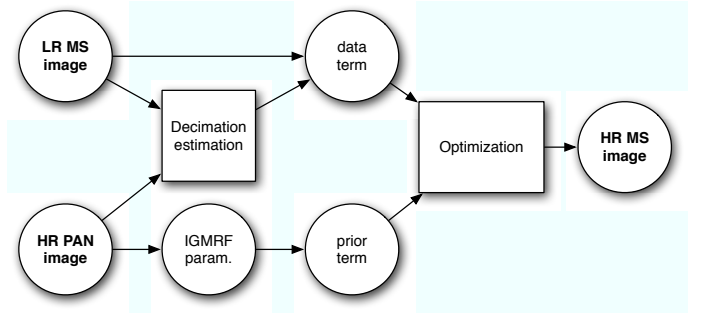


Fig. 1. A general scheme of the data fusion for an MS and a Pan image. Here LR and HR represent high resolution and low resolution, respectively.

address the problem of ill-posedness. What we present in this paper differs from their work. Our image formation model is based on the restoration framework which properly models the aliasing present in the low spatial resolution MS images due to undersampling. We then solve the ill-posedness of the problem by using the Bayesian approach, in particular by formulating the problem as MAP estimation. Our objective function (cost function) does not explicitly include the high resolution estimate derived from the Pan image as used in [47], as this would cause spectral distortion since the Pan data has low spectral resolution. We would like to mention here that both the approaches are MRF based and use a combination of prior model and data term. However, the two works differ significantly in their implementation.

The outline of the paper is as follows. In section II, we briefly explain the proposed approach. In Section III, the forward model for the low spatial resolution MS image formation is presented. The high resolution image field as an IGMRF model and the model parameters estimation are the subject of section IV. The MAP based approach to enhance the spatial resolution of MS images in order to obtain the fused MS images is discussed in section V. Experimental results are presented in section VI and section VII provides conclusions of our work.

II. Block diagram description of the Proposed method.

The method for the proposed multiresolution fusion can be explained using the block schematic shown in Figure 1. A low resolution MS image is modeled as an aliased and noisy version of the corresponding high spatial and spectral resolution fused image. It may be noted that the block diagram shows the fusion process for the n^{th} low resolution image and the Pan image with the result Z_n corresponding to the fused MS image. We thus obtain one fused image for each of the MS images. A bicubically interpolated image of the corresponding MS image is used to initialize the iterative optimization algorithm. The decimation matrix, applied to the high resolution estimate, and the available low resolution MS image are used to form the data fitting term (likelihood term). One could infer the decimation matrix using the available high resolution Pan image. However, we do not address this problem in this paper and we use a fixed decimation matrix as used in [46]. In order to solve the problem using MAP we need a prior model for regularization. This is done by modeling each of the high spatial resolution MS images (to be estimated) as an IGMRF. The IGMRF parameters are learned

from the Pan image and are used on the high resolution MS estimate to form the prior term. A suitable optimization scheme is then used to minimize the cost function containing data fitting term and prior term in order to estimate the unknown high resolution MS image. The optimization is carried out separately for each of the MS images and we obtain high spatial and spectral resolution MS image for each band. Note that the same IGMRF parameters are used for each of the MS images as we are learning the spatial correlation among the pixels which is assumed to be the same for all the high resolution MS images. It may be mentioned here that this assumption requires images registered before the fusion process. Since we learn the spatial properties and not the spectral characteristics we expect the spectral properties to be preserved in the fused MS images.

III. Forward Model

The proposed multiresolution fusion problem is cast in a reconstruction framework. There are p observed low resolution MS images ($Y_n, n = 1, 2, \dots, p$), each captured with a different spectral band, of size $M_1 \times M_2$ pixels and a single Pan image Z captured with a high spatial resolution of size $qM_1 \times qM_2$. This is also the size of each of the fused images ($Z_n, n = 1, 2, \dots, p$). Here q represents the decimation factor (aliasing factor) and is an integer.

Let \mathbf{z} represent the available high resolution Pan image in lexicographical order. Given the high resolution MS image \mathbf{z}_n (lexicographically ordered), the corresponding low resolution image can be modeled as the decimated and noisy version of this high resolution image. If \mathbf{y}_n is the n^{th} observed image containing pixels from the low spatial resolution MS image then we can write:

$$\mathbf{y}_n = D_n H_n \mathbf{z}_n + \mathbf{v}_n, \quad n = 1, 2, \dots, p. \quad (1)$$

Here D_n is the decimation matrix of size $M_1 M_2 \times q^2 M_1 M_2$ and H_n is the blurring matrix of size $q^2 M_1 M_2 \times q^2 M_1 M_2$ which is assumed to be an identity matrix. \mathbf{v}_n is the $M_1 M_2 \times 1$ noise vector which is zero mean independent and identically distributed (i.i.d.) process with variance σ_v^2 . Now the problem is to estimate \mathbf{z}_n given the observation \mathbf{y}_n , which has clearly many solutions and hence it is ill-posed. We need a proper regularization to obtain better solution by restricting the solution space.

It can be seen that when a fixed decimation matrix as used by the super-resolution community is employed it has the following form as given in [48]

$$D = \frac{1}{q^2} \begin{bmatrix} 11\dots 1 & & & \mathbf{0} \\ & 11\dots 1 & & \\ & & \ddots & \\ \mathbf{0} & & & 11\dots 1 \end{bmatrix}. \quad (2)$$

For example, for a decimation factor of $q = 2$ and with high resolution fused image of size 4×4 i.e., 16×1 lexicographically ordered, the D matrix is of size 4×16 and can be written as

$$D = \frac{1}{4} \begin{bmatrix} 1100110000000000 \\ 0011001100000000 \\ 0000000011001100 \\ 0000000000110011 \end{bmatrix}. \quad (3)$$

This decimation model simulates the integration of light intensity that falls on the high resolution detector and the decimation process is represented by the matrix D which has the structure given in (2). This shows that the low resolution image intensity is the average of corresponding high resolution intensities over a neighborhood of q^2 pixels and corrupted with an additive noise. That is, all the non zero entries in the (3) have a constant value of $\frac{1}{q^2}$. We mention here that the warping matrix is not considered in equation (1) as the considered images are registered.

IV. IGMRF Prior Model

As discussed in section III, we propose to solve the multiresolution fusion problem as an ill-posed inverse problem, therefore it needs a suitable regularization scheme in order to make it better posed. The regularization can be carried out assuming a proper prior density for the unknown fused image. We plan to model the fused image in such a way that the model parameters can be used in the regularization for the purpose of obtaining a better solution. In the area of image processing and computer vision many researchers use Markov Random Fields (MRF) as convenient way of modeling the contextual entities such as image pixels, depth field and other correlated features. This is obtained by mathematically representing the mutual influence among such entities over a spatial neighborhood. An MRF prior for the unknown image can be described by using a energy function U expressed in the Gibbsian density given by

$$P(\mathbf{z}_n) = \frac{1}{Z_{n\theta}} \exp(-U(\mathbf{z}_n)). \quad (4)$$

Here \mathbf{z}_n is the unknown image to be estimated and $Z_{n\theta}$ represents the normalizing constant known as partition function. One can choose U as a quadratic form with a single global parameter, assuming that the images are globally smooth. However, a more efficient model would be to choose U such that only the homogeneous regions are smooth and discontinuities are preserved in the form of edges. To get this edge preserving regularization researchers have used MRF's with discrete line fields [49], [50]. However, accurate estimation of these line field parameters is a very difficult task and computationally demanding. Also the energy function becomes non-quadratic and hence needs costly optimization methods such as simulated annealing in order to estimate the unknown image. To get the edge preserving regularization, it is possible to use non quadratic ϕ -function, as introduced [51] with a single parameter estimated globally [52], or few parameters estimated considering small homogeneous areas extracted from a large-size image [53]. In practice a real satellite image can seldom be represented by homogeneous models as they are made up of different textures with sharp edges as well as constant areas. Hence the prior has to be chosen such that the prior parameter adapts to the local structure of the image yielding less noisy result in the homogenous areas, and also preserve the sharp details. This motivates us to choose an inhomogeneous Gaussian MRF (IGMRF) to model the unknown image.

While using the IGMRF prior, the authors in [54] used the following energy function U in order to model the reconstructed

solution Z_n while solving the satellite image deblurring problem.

$$U(Z_n) = \sum_i \sum_j \left\{ \begin{aligned} & b_{i,j}^x (Z_n(i-1, j) - Z_n(i, j))^2 \\ & + b_{i,j}^y (Z_n(i, j) - Z_n(i, j-1))^2 \end{aligned} \right\}. \quad (5)$$

Here $b_{i,j}^x$ and $b_{i,j}^y$ are the spatially adaptive parameters of the prior model, with respect to columns and rows. As proposed in [54], approximate Maximum Likelihood estimates can be derived using two assumptions: the independence between pixel gradients, and the availability of complete data, or ground truth. In this case the optimal value has the form $\hat{b} = 1/4g^2$ if g is an image gradient. We approximate the ground truth by the Pan image, neglecting the contribution of the noise. We do not allow the regularization parameters to exceed a predefined value in order to avoid computational issues, that could otherwise arise when the gradient values tend to zero. Thus the derived prior parameters are computed using the following expressions.

$$\begin{aligned} \hat{b}_{i,j}^x &= \frac{1}{\max(4(Z_{i-1,j} - Z_{i,j})^2, 4)}, \\ \hat{b}_{i,j}^y &= \frac{1}{\max(4(Z_{i,j-1} - Z_{i,j})^2, 4)}. \end{aligned} \quad (6)$$

It can be observed that the variable b represents a continuous line process [55] with low values of b indicating an edge between two pixels. In the above energy function, the authors model the spatial dependency at a pixel location by considering a first order neighborhood related to edges in the horizontal and vertical directions. However, in practice the edges in the reconstructed image are not restricted to the two directions only. In order to take care of diagonal edges as well we consider a second order neighborhood and modify the energy function as follows.

$$U(Z_n) = \sum_i \sum_j \left\{ \begin{aligned} & b_{i,j}^x (Z_n(i, j) - Z_n(i-1, j))^2 \\ & + b_{i,j}^y (Z_n(i, j) - Z_n(i, j-1))^2 \\ & + b_{i,j}^u (Z_n(i, j) - Z_n(i-1, j-1))^2 \\ & + b_{i,j}^v (Z_n(i, j) - Z_n(i-1, j+1))^2 \end{aligned} \right\}, \quad (7)$$

where $b_{i,j}^u$ and $b_{i,j}^v$ represent the additional parameters for considering the interactions in the diagonal directions. We thus have four parameters at each pixel location instead of two as used in [54]. Thus $\{b_{i,j}^x, b_{i,j}^y, b_{i,j}^u, b_{i,j}^v\}$ form the parameter vector at each location.

These parameters of the prior model are unknown as the true high resolution MS images are unavailable and are to be estimated. To solve this ambiguity we propose to use the available high resolution Pan image of the same scene, which is assumed to be acquired at the same time in order to learn the IGMRF parameters so that they can be used to improve the solution. These parameters are estimated using the approach as discussed in [54] where the authors use a Maximum Likelihood (ML) estimator with the complete data and use a simple approximation of the local variance in order to reduce the computational complexity. The prior parameters are estimated using the following expressions.

$$\hat{b}_{i,j}^x = \frac{1}{\max(8(Z_{i-1,j} - Z_{i,j})^2, 8)},$$

$$\begin{aligned} \hat{b}_{i,j}^y &= \frac{1}{\max(8(Z_{i,j-1} - Z_{i,j})^2, 8)}, \\ \hat{b}_{i,j}^u &= \frac{1}{\max(8(Z_{i-1,j-1} - Z_{i,j})^2, 8)}, \\ \hat{b}_{i,j}^v &= \frac{1}{\max(8(Z_{i-1,j+1} - Z_{i,j})^2, 8)}. \end{aligned} \quad (8)$$

It may be noted that in Eq. (5, 7), Z_n represents the n^{th} fused image while Z in Eq. (6, 8) corresponds to the available high resolution Pan image.

V. MAP estimation

We now explain how the fusion can be performed using the MAP estimation so that we obtain the high spatial and spectral resolution MS images. It may be noted that the MAP estimation is done separately for each of the MS bands. The IGMRF model on the fused image serve as the prior for the MAP estimation. The model parameters are estimated from the available high spatial resolution Pan image and the data fitting term contains the aliasing matrix. In order to use maximum *a posteriori* (MAP) estimation to obtain the fused MS image \mathbf{z}_n given the MS and Pan observations, we need to obtain the estimate as $\hat{\mathbf{z}}_n = \arg \max_{\mathbf{z}_n} P(\mathbf{z}_n/\mathbf{y}_n)$. Using the Bayes' rule we can write

$$P(\mathbf{z}_n/\mathbf{y}_n) = P(\mathbf{y}_n/\mathbf{z}_n)P(\mathbf{z}_n).$$

Now taking the log and considering that the random variables in \mathbf{v}_n are independent we can write

$$\hat{\mathbf{z}}_n = \arg \max_{\mathbf{z}_n} \left[\log P(\mathbf{y}_n/\mathbf{z}_n) + \log P(\mathbf{z}_n) \right].$$

Finally, using the eqs. (1) and (4) the final cost function to be minimized can be expressed as

$$\hat{\mathbf{z}}_n = \arg \min_{\mathbf{z}_n} \left[\frac{\|\mathbf{y}_n - D_n \mathbf{z}_n\|^2}{2\sigma_v^2} + U(\mathbf{z}_n) \right]. \quad (9)$$

It can be seen that the above cost function is quadratic (not only convex) therefore the most computationally efficient way to optimize it would be the conjugate gradient method, however we chose to implement a simple gradient descent algorithm in our tests, for the sake of simplicity. Since the model parameter values $b_{i,j}^x$, $b_{i,j}^y$, $b_{i,j}^u$, and $b_{i,j}^v$ have been already estimated, a solution to the above equation can be easily obtained.

In order to speedup the convergence, the initial estimate $\mathbf{z}_n^{(0)}$ is obtained as the bicubically interpolated version of the multispectral image \mathbf{y}_n . The minimization is carried out independently for each of the multispectral (MS) images using the same parameter set learned from the Pan image resulting in the fused high spatial and spectral resolution multispectral images.

VI. Experimental Results and Performance Comparison

In this section we demonstrate the effectiveness of the proposed approach by conducting experiments on the synthetic data as well as on the real images captured by the satellite sensors. First we demonstrate the working of our model by conducting experiments on simulated images for a decimation factor of 2. We next illustrate how our model works on a real satellite

data by reconstructing a high resolution image from its decimated and noisy version. Finally we show the performance of the proposed approach in terms of both the perceptual as well as quantitative measures by conducting the experiments on Quickbird satellite images with a spatial resolution difference of 4 between the available Pan and MS images. We choose this data set in order to compare our results with those presented in [45]. The experiments were conducted on images acquired over the same geographical area and at the same time. The results are compared with the other methods based on the perceptual differences as well as by using quantitative measures. In order to test the quality of results by using quantitative measures, we conduct the experiments on spatially degraded versions so that the fused results can be compared with the true MS images.

A. Experimentation on a Synthetically Generated Image

Here we consider the verification of our model for the proposed fusion method by considering a synthetically generated data. To start with, we generate a checkerboard image and treat it as a high spatial resolution image. The observed low resolution image is then formed by decimation and addition of an independent and identically distributed (i.i.d) Gaussian noise of variance $\sigma_v^2 = 0.0004$. This is the noise variance when the maximum and minimum pixel intensities are 1 and 0, respectively. Now the problem here is to estimate the high resolution image from its degraded version. Figure 2(a) shows the original high resolution image. In Figure 2(b) we display the decimated and noisy version of the same. A decimation factor of 2 was used and the decimation is obtained by considering the average of four high resolution pixel intensities in order to obtain a single low resolution pixel intensity [48]. The IGMRF parameters estimated from the high resolution image are then used in the cost function (Eq. (9)). A fixed step size of 0.001 was used for this experiment while optimizing using the gradient descent algorithm that converged in less than 100 iterations. Figure 2(c) shows the estimated high resolution image using the proposed MAP based approach. It can be seen that in the reconstructed image the noise is very much reduced and the edge details are sharper. In order to show how well the model captures the spatial dependency in the form of IGMRF parameters we compare the result with the bicubically interpolated version of the low resolution observation (see Figure 2(d)) which appears blurred and noisy. This experiment demonstrates the working of our model and also clarifies that the method is capable of performing image fusion in general. It is important to mention here that the above experiment do not validate our prior model, rather it verifies the working of the model.

B. Experimental Illustration with a Single image

The objective of this experimentation is to test the efficacy of the proposed method when we consider a real satellite image as the test image and try to recover this image from its degraded version. We choose a single panchromatic image acquired using the Ikonos satellite (1 m \times 1 m spatial resolution), and subsample it to 4 m \times 4 m to minimize the effects of degradations such as blur and noise. The observed low resolution image is then constructed as discussed in the previous section (decimation factor $q=2$). However, in this case we add noise of higher

variance ($\sigma_v^2 = 0.0025$) to the decimated version of the test image in order to test our algorithm for noisy conditions. Figures 3(a, b, c and d) show the images for this experiment. The result shown in Figure 3(c) indicates that the proposed approach reconstructs the high resolution image very well even when the data has more noise.

C. Experimentations on Quickbird Images

In the previous two experiments the IGMRF parameters were estimated from the available high resolution image. However, when one captures the remotely sensed images the MS images are at lower spatial resolution (high spectral resolution) while the Pan image is captured at high spatial resolution (low spectral resolution). We can then obtain the high resolution fused MS images by using the IGMRF parameters estimated on the Pan image.

In this subsection we consider fusing the MS images of Quickbird satellite and the Pan image captured over the Malpensa area, Italy. The Quickbird data set consists of four MS bands at a spatial resolution of 2.4 m \times 2.4 m and a coregistered Pan image with a spatial resolution of 0.6 m \times 0.6m (giving a spatial resolution difference or decimation factor of 4). As already mentioned these images are degraded to 9.6 m \times 9.6 m and 2.4 m \times 2.4 m, respectively so that after the fusion the MS images have a resolution of 2.4 m \times 2.4 m. The degradation for each pixel is obtained by taking the average over four pixels of the Pan image and then adding the noise. It may be noted that this decimation is necessary since we are conducting the experiments on the degraded versions. Since these degraded images form the observed images we use the degraded Pan image for estimating the IGMRF parameters as it now represent the available high resolution data. The fused images obtained using the proposed method are then used for quality assessment by comparing them with the true (undegraded) MS images. The size of the true Pan and MS data are 512 \times 512 and 128 \times 128, respectively, and after degrading them in order to conduct the experiment they are of size 128 \times 128 and 32 \times 32, respectively. We learn four matrices of size 128 \times 128 each for representing b^x , b^y , b^u , and b^v parameters using the degraded Pan image. While estimating these values using (Eq. 8) we set a value of $\frac{1}{8}$ (instead of a very high value) whenever the neighboring pixel intensities are same i.e., whenever the spatial gradient becomes zero. Thus we set a minimum spatial difference of 1 for practical reasons. This avoids obtaining high regularization parameter values that would slow down the optimization. This ensures that the pixels with zero intensity difference are weighted almost the same as those with the small intensity difference (in this case with a difference of 1). We compare the results of our approach with the HPF method, the Gram-Schmidt (GS) approach, and the model based approach proposed in [45]. For the proposed method the spatial dependency captured by the IGMRF parameters were used in the cost function during minimization. The gradient descent algorithm converged in less than 100 iterations with a fixed step size of 0.001. The processing time on a 2GHz PowerPC G5 processor was a few seconds. It may be mentioned here that most of the fusion methods in the literature do not use iterative approaches and may have a slight advantage over the proposed approach in terms of computational complexity. How-

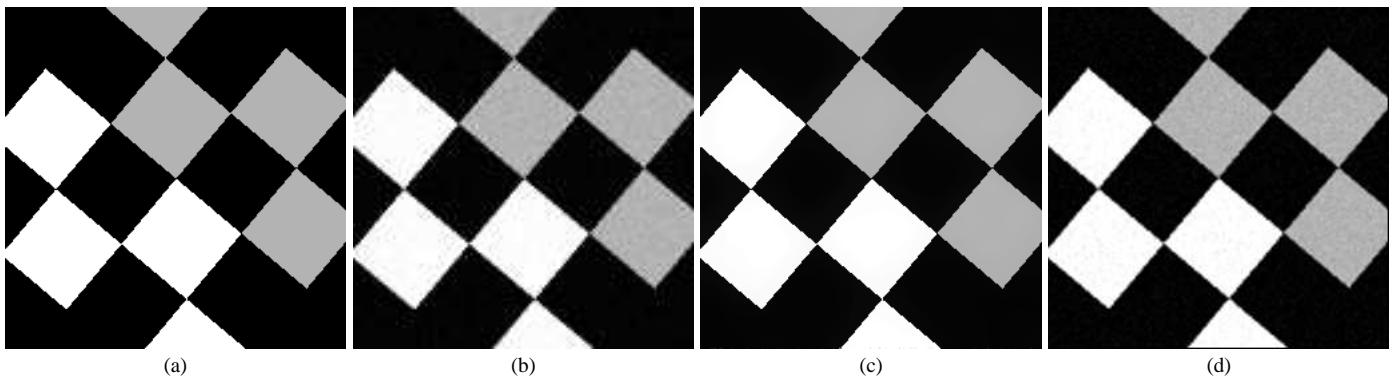


Fig. 2. Results for a synthetically generated and degraded checkerboard image. (a) 256×256 pixels high resolution checkerboard image. (b) Decimated and noisy version of (a) using a noise variance of 0.0004. (c) Estimated high resolution image using the proposed approach. (d) Bicubically interpolated image of (b).

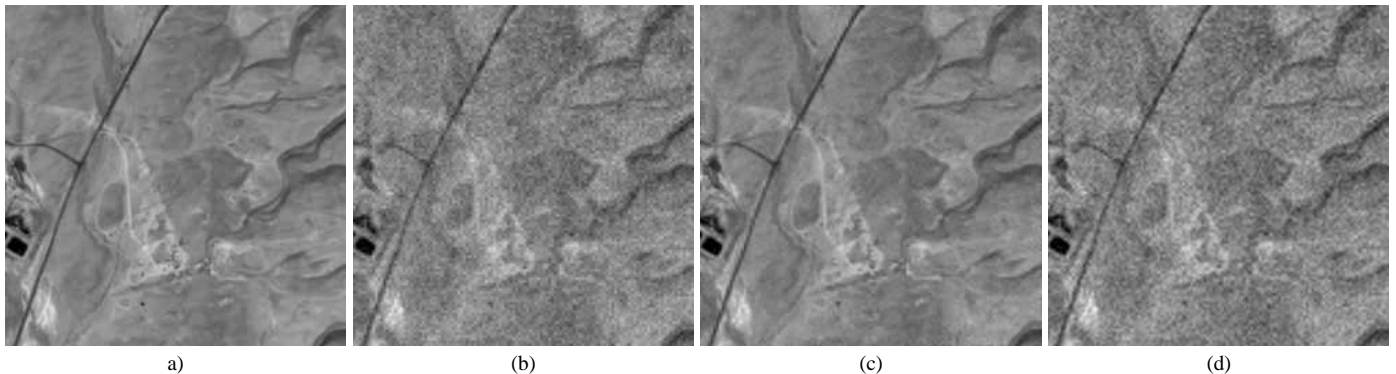


Fig. 3. Deblurring results on a grayscale image (subsampled Ikonos image of Gooseneck © Space Imaging, $4 \text{ m} \times 4 \text{ m}$ spatial resolution). (a) 256×256 pixels high resolution image. (b) Decimated and noisy version of (a) using a noise variance $\sigma_v^2 = 0.0025$. (c) Estimated high resolution image using the proposed approach. (d) Bicubically interpolated image of (b).

ever, the fusion approaches proposed in the literature directly operate on the Pan image intensity values, thus introducing the spectral distortion. Also the up sampling of the MS images to match the size of the Pan image during the fusion process introduces aliasing in these methods. These are properly taken care in the proposed approach by using the learned IGMRF parameters from the Pan image (instead of directly using the Pan values) and appropriately modeling the aliasing.

In order to demonstrate the efficacy of our approach, we first consider the fusion of the MS bands 4, 3, 2, lying in the visible and near infra red regions. This spectral range lie within the spectral range of Pan image. In Figure 4 we display the results using the color composites of the fused 4, 3, and 2 bands. Figure 4(a) shows the color composite for true MS bands 4, 3, 2. The fusion results obtained using the HPF method, the Gram-Schmidt (GS) approach, and the autoregressive (AR) model based approach are shown in Figures 4(b, c, and d). The result obtained using the proposed IGMRF model based approach is depicted in Figure 4(e). We observe that the high frequency details at various regions are better preserved in Figure 4(e), indicating the proper modeling of aliasing as well as the edge details in the form of IGMRF prior. The image looks similar to the one displayed in Figure 4(a), the true MS color composite. The result obtained using HPF method exhibits noise amplification because of the high pass filtering action. In the proposed method this is properly taken care by using the calculated IGMRF parameters b^x , b^y , b^u , and b^v at each pixel. The results using the Gram-Schmidt (GS) and AR model based approaches (see Fig-

ure 4(c, d)) lack the sharpness. The use of homogeneous AR parameter tends to make the result more smooth as few parameters are estimated using the least squares approach considering small neighborhoods over the entire pan image. In this case the number of estimated parameters depends on the neighborhood size and the computation cost increases with the increase in the size of the neighborhood. It may be mentioned here that in [45], the performance increase was negligible with the use of more than twenty four parameters.

In the second set of experiments, we repeated the previous trials by considering spectral bands 3, 2 and 1. The different parameters used in the gradient descent algorithm were kept the same as in the previous experiment. The results for different approaches are shown in Figure 5(a, b, c, d) and the result for the proposed method is displayed in Figure 5(e). Once again we observe that the proposed approach works well for a different spectral bandwidth also.

In order to show the comparative edge over the other approaches in terms of quantitative assessment, we use the following measures as used in [56]. These are

1. Standard deviation of the original and the fused images.
2. Definition of the original and the fused images.
3. Distortion extent of the fused images.
4. Deviation index of the fused images.
5. Correlation coefficient between the original and the fused images.
6. Mean squared error (MSE) between the original and the fused images.

Image	RASE	ERGAS
HPF (coregistered)	1.038	4.567
GS (coregistered)	0.571	2.385
AR (Symmetric)	0.372	1.580
AR (Asymmetric)	0.452	1.896
Proposed	0.476	0.857

TABLE III

GLOBAL QUANTITATIVE ASSESSMENT OF THE FUSION RESULTS PROVIDED BY THE CONSIDERED TECHNIQUES IN TERMS OF RASE AND ERGAS MEASURES FOR BANDS 4, 3, 2 OF THE QUICKBIRD DATA SET.

We also compare our approach using RASE (*relative average spectral error*) and ERGAS (*erreur relative globale adimensionnelle de synthèse*) indices [21].

It must be mentioned here that the standard deviation and the definition indicate how well the spatial characteristics are preserved in the fused image whereas the other measures show the comparison for spectral information. For a better fusion we expect that both the standard deviation and the definition should be either high or close to their true values and the correlation coefficient should approach unity. The distortion extent, the deviation index, and the mean squared error (MSE) should be low. These results are shown in Tables I and II. The following conclusions can be drawn from these tables. We observe that the overall performance of the proposed approach is better when compared to other methods both in terms of the spectral and the spatial measures. As required the standard deviation and the definition are high for bands 1 – 4 for the proposed method. For the proposed method the MSE for the band 1 is slightly superior when compared to GS and HPF (refer to Table I) and it is superior for band 4 when compared to AR model based approach (see Table II). However, it performs better in terms of deviation index and correlation coefficient indicating that the spectral properties are better preserved. One can observe that for Band 2 the proposed method performs very well indicating better performance in terms of all the quantitative measures. Finally, we show the quantitative measures in terms of RASE and ERGAS indices in Table III. Here we consider the comparison using the coregistered bands since registration is necessary for the accurate estimation of the IGMRF parameters for the proposed approach. The comparison is shown for the coregistered bands 4, 3, and 2. The comparison with the AR method is shown for both the symmetric case where eight parameters are estimated considering the symmetry in the horizontal and the diagonal directions and the asymmetric case where twenty four parameters are estimated. From the table it is clear that although the method gives slightly higher RASE value as compared to AR based approach the value of the ERGAS is considerably reduced when compared to other all the other methods. We conclude that a slight inferior performance in few of the indices may be due to the approximation made in estimating the IGMRF parameters and the probable lack of sufficient prior information. It may be mentioned here that the computational cost increases to a large extent when we attempt to estimate the true IGMRF parameters.

VII. Conclusions

We have described a method for the multiresolution fusion of remotely sensed images that do not directly use the Pan pixel intensities, but exploits the spatial correlation among pixels in the form of IGMRF parameters estimated from the Pan image. The low spatial resolution MS images are modeled as the decimated and noisy versions of their corresponding high resolution images. Each of the fused MS images are separately modeled as IGMRFs to provide the necessary prior and an MAP estimation is used to obtain the fused images. The advantage of the proposed approach is that the high resolution texture for the fused images are properly learned in the form of IGMRF parameters. The method performed very well in terms of both the spectral and spatial fidelity when compared to other standard approaches.

In this work we present results from the Pan and MS images acquired using the Quickbird satellite. Our future work involves fusion of Pan and MS images captured using different sensors at different times. Our future work also involves the estimation of the decimation matrix, and improvements on the estimation of IGMRF parameters using the dependencies between Pan and MS bands, in order to better adapt Pan-derived parameters to each MS band. The proposed work uses multispectral images for fusion. In our future work we would like to look at the fusion of hyperspectral images obtained using the Airborne Visible/Infrared Imaging Spectrometer (AVIRIS) so that one can obtain high spatial and spectral resolution images for thousands of narrow spectral bands.

VIII. Acknowledgments

The Authors would like to thank the anonymous reviewers and the editor for their constructive comments and suggestions that have greatly improved the contents and scope of the paper. This work was partially funded by the French Research Agency (ANR) as part of the SpaceFusion project (Program “*Jeunes Chercheurs 2005*” Grant # *JC05_41500*). The research was initiated while Manjunath Joshi was an invited professor at LSIT (UMR 7005 CNRS-University of Strasbourg), France.

REFERENCES

- [1] L. Wald, “Some terms of reference in data fusion,” *IEEE Trans. Geosci. Remote Sensing*, vol. 37, no. 3, pp. 1190–1193, 1999.
- [2] P. K. Varshney, “Multisensor data fusion,” *Electron. Commun. Eng. J.*, pp. 245–263, 1997.
- [3] D. L. Hall and J. Llinas, “An introduction to multisensor data fusion,” *Proc. IEEE*, vol. 85, no. 1, pp. 6–23, 1997.
- [4] A. H. J. M. Pellemans, R. W. L. Jorrdans, and R. Allewijn, “Merging multispectral and panchromatic spot images with respect to the radiometric properties of the sensor,” *Photogrammetric Engineering and Remote Sensing*, vol. 59, no. 1, pp. 81–87, 1993.
- [5] R. Hayden, G. W. J. Henkel, and J. E. Bare, “Application of the ihs color transform to the processing of multisensor data and image enhancement,” in *Proc. International Symposium on Remote sensing of arid and semi-arid lands*, Cairo, Egypt, 1982, pp. 599–616.
- [6] V. Jim, “Multispectral imagery band sharpening study,” *Photogrammetric Engineering and Remote Sensing*, vol. 62, no. 9, pp. 1075–1083, 1996.
- [7] Hong Jing and Liudi Liu, “Color space conversion methods’ applications to the image fusion,” *Optical Technology*, , no. 4, pp. 44–48, 1997.
- [8] P. S. Jr. Chavez, S. C. Sides, and J. A. Anderson, “Comparison of three different methods to merge multiresolution and multispectral data: Landsat TM and SPOT panchromatic,” *Photogrammetric Engineering and Remote Sensing*, vol. 57, no. 3, pp. 295–303, 1991.
- [9] L. Wald, T. Ranchin, and M. Mangolini, “Fusion of satellite images of different spatial resolutions: assessing the quality of resulting images,”



Fig. 4. Fusion results of degraded MS bands 4, 3, and 2 color composite (a) 128×128 pixels true MS color composite at $2.4 \text{ m} \times 2.4 \text{ m}$ spatial resolution, (b) HPF fused MS ($2.4 \text{ m} \times 2.4 \text{ m}$), (c) fusion using Gram-Schmidt (GS) method ($2.4 \text{ m} \times 2.4 \text{ m}$), (d) Homogeneous AR model based approach ($2.4 \text{ m} \times 2.4 \text{ m}$), (e) Fusion using the estimated IGMRF parameters from the high resolution Pan image.

Image	Standard Deviation	Definition	Distortion extent	Deviation index	Correlation coefficient	MSE
MS-Band 1	53.166	14.461	-	-	-	-
HPF	46.656	13.427	19.385	0.076	0.851	0.012
GS	43.530	12.183	18.361	0.074	0.875	0.011
AR Model	64.152	22.830	23.919	0.098	0.850	0.018
Proposed	58.141	17.838	18.669	0.073	0.855	0.014

(A)

Image	Standard Deviation	Definition	Distortion extent	Deviation index	Correlation coefficient	MSE
MS-Band 2	95.098	26.292	-	-	-	-
HPF	81.762	21.972	33.893	0.096	0.859	0.017
GS	78.767	23.327	31.558	0.091	0.886	0.015
AR Model	88.910	24.310	27.871	0.079	0.901	0.013
Proposed	93.816	27.000	27.256	0.078	0.917	0.011

(B)

TABLE I

QUANTITATIVE COMPARISON OF THE FUSION RESULTS USING THE QUICKBIRD DATA SET: (A) BAND 1, (B) BAND 2



Fig. 5. (a) 128×128 pixels true MS color composite at $2.4 \text{ m} \times 2.4 \text{ m}$ spatial resolution (3, 2, and 1 color composite), (b) HPF fused MS ($2.4 \text{ m} \times 2.4 \text{ m}$), (c) fusion using Gram-Schmidt (GS) method ($2.4 \text{ m} \times 2.4 \text{ m}$), (d) Homogeneous AR model based approach ($2.4 \text{ m} \times 2.4 \text{ m}$), (e) Fusion using the estimated IGMRF parameters from the high resolution Pan image.

Image	Standard Deviation	Definition	Distortion extent	Deviation index	Correlation coefficient	MSE
MS-Band 3	82.169	22.579	-	-	-	-
HPF	70.182	17.577	28.934	0.123	0.867	0.024
GS	69.243	21.007	26.994	0.117	0.890	0.020
AR Model	81.848	23.543	25.018	0.113	0.895	0.021
Proposed	84.558	25.792	25.087	0.107	0.912	0.017

(A)

Image	Standard Deviation	Definition	Distortion extent	Deviation index	Correlation coefficient	MSE
MS-Band 4	91.441	25.718	-	-	-	-
HPF	77.209	18.137	32.700	0.109	0.861	0.017
GS	76.883	20.641	32.236	0.107	0.873	0.015
AR Model	86.320	24.084	30.323	0.096	0.885	0.013
Proposed	90.528	26.060	29.391	0.094	0.891	0.014

(B)

TABLE II

QUANTITATIVE COMPARISON OF THE FUSION RESULTS USING THE QUICKBIRD DATA SET: (A) BAND 3, (B) BAND 4

- Photogrammetric Engineering and Remote Sensing*, vol. 63, no. 6, pp. 691–699, 1997.
- [10] M. Ehlers, “Multisensor image fusion techniques in remote sensing,” *ISPRS Journal of Photogrammetry and Remote Sensing*, vol. 46, pp. 19–30, 1991.
 - [11] H. Yesou, Y. Besnus, and Y. Rolet, “Extraction of spectral information from landsat TM data and merger with SPOT panchromatic imagery—a contribution to the study of geological structures,” *ISPRS Journal of Photogrammetry and Remote Sensing*, vol. 48, no. 5, pp. 23–36, 1993.
 - [12] H. Li, B. S. Manjunath, and S. K. Mitra, “Multisensor image fusion using the wavelet transform,” *Graphical Models and Image Processing*, vol. 27, no. 3, pp. 235–244, 1995.
 - [13] D. A. Yocky, “Image merging and data fusion by means of the discrete two dimensional wavelet transform,” *Journal of Optical Society of America*, vol. 12, no. 8, pp. 1834–1841, 1995.
 - [14] E. Yu and R. Wang, “Fusion and enhancement of the multispectral image with wavelet transform,” *Computer Engineering and Science*, vol. 23, no. 1, pp. 47–50, 2001.
 - [15] J. Nunez, “Multiresolution-based image fusion with additive wavelet decomposition,” *IEEE trans. on Geoscience and Remote Sensing*, pp. 1204–1211, May 1999.
 - [16] J. Nunez, X. Otazu, O. Fors, A. Prades, V. Pala, and R. Arbiol, “Multiresolution based image fusion with additive wavelet decomposition,” *IEEE Trans. on Geoscience and Remote Sensing*, vol. 37, pp. 1204–1211, May 1999.
 - [17] Y. Chibani and A. Houacine, “Model for multispectral and panchromatic image fusion,” in *Proc. SPIE Image and Signal Processing for Remote sensing*, 2000, pp. 238–244.
 - [18] A. Garzelli, G. Bennelli, M. Barni, and C. Magini, “Improving wavelet based merging of panchromatic and multispectral images by contextual information,” in *Proc. SPIE Image and Signal Processing for Remote sensing*, 2000, pp. 82–91.
 - [19] B. Aiuzzi, L. Alparone, S. Baronti, and A. Garzelli, “Context driven fusion of high spatial and spectral resolution images based on oversampled multiresolution analysis,” *IEEE trans. on Geoscience and remote sensing*, vol. 40, no. 10, pp. 2300–2312, October 2002.
 - [20] M. Choi, R. Y. Kim, M. R. Nam, and H. O. Kim, “Fusion of multispectral and panchromatic satellite images using the curvelet transform,” *IEEE Trans. Geosci. Remote Sensing*, vol. 2, no. 2, pp. 136–140, April 2005.
 - [21] M. G. Audicana, J. L. Saleta, R. Garcia Catalàn, and R. Garcia, “Fusion of multispectral and panchromatic images using improved IHS and PCA mergers based on wavelet decomposition,” *IEEE Trans. Geosci. Remote Sensing*, vol. 42, no. 6, pp. 1291–1299, June 2004.
 - [22] T. Ranchin, B. Aiuzzi, L. Alparone, S. Baronti, and L. Wald, “Image fusion - the ARSIS concept and some successful implementation schemes,” *ISPRS Journal of Photogrammetry and Remote Sensing*, vol. 58, no. 1-2, pp. 4–18, June 2003.
 - [23] Aiuzzi B. L. Alparone, S. Baronti, and M. Selva, “MS + Pan image fusion by enhanced Gram-Schmidt spectral sharpening,” in *proceedings of the 26th EARSeL Symposium “New strategies for European Remote sensing*, 26-31, May 2006, Varsovie, Pologne.
 - [24] L. Alparone, S. Baronti, A. Garzelli, and F. Nencini, “A global quality measurement of pan-sharpened multi-spectral imagery,” *IEEE Trans. Geosci. Remote Sensing Lett.*, vol. 1, no. 4, pp. 313–317, October 2004.
 - [25] M. Choi, “A new intensity-hue-saturation fusion approach to image fusion with a tradeoff parameter,” *IEEE Trans. Geosci. Remote Sensing*, vol. 44, no. 6, pp. 1672–1682, June 2006.
 - [26] M Lillo Saavedra, M. C. Gonzalo, A. Arquero, and E. Martinez, “Fusion of multispectral and panchromatic satellite imagery based on tailored filtering in the Fourier domain,” *International Journal of remote sensing*, vol. 26, no. 6, pp. 1263–1268, March 2005.
 - [27] X. Otazu, M. Gonzalez-Audicana, O. Fors, and J. Nunez, “Introduction of sensor spectral response into image fusion methods. application to wavelet-based methods,” *IEEE Trans. Geosci. Remote Sensing*, vol. 43, no. 10, pp. 2376–2385, 2005.
 - [28] W. Shi, C. Zhu, Y. Tian, and J. Nichol, “Wavelet-based image fusion and assessment,” *International Journal of Applied Earth Observation and Geoinformation*, vol. 6, no. 3-4, pp. 241–251, March 2005.
 - [29] V. Tsagaris, V. Anastassopoulos, and G. A. Lampropoulos, “Fusion of hyperspectral data using segmented PCT for color representation and classification,” *IEEE Trans. Geosci. Remote Sensing*, vol. 43, no. 10, pp. 2365–2375, October 2005.
 - [30] Z. Wang, D. Ziou, C. Armenakis, D. Li, and Q. Li, “A comparative analysis of image fusion methods,” *IEEE Trans. Geosci. Remote Sensing*, vol. 43, no. 6, pp. 81–84, June 2005.
 - [31] Y. Zheng, E. A. Essock, B. C. Hansen, and A. M. Haun, “A new metric based on extended spatial frequency and its application to DWT based fusion algorithms,” *Information fusion*, vol. 8, no. 2, pp. 177–192, April 2005.
 - [32] L. Alparone, L. Wald, J. Chanussot, P. Gamba, and L. Mann Bruce, “Comparison of pansharpening algorithms: Outcome of the 2006 GRS-S data fusion contest,” *IEEE trans. on Geoscience and remote sensing*, vol. 45, no. 10, pp. 3012–3021, October 2007.
 - [33] K. A. Kalpoma and J. Kudoh, “Image fusion processing for ikonos 1-m color imagery,” *IEEE trans. on Geoscience and remote sensing*, vol. 45, no. 10, pp. 3075–3086, October 2007.
 - [34] B. Aiuzzi, S. Baronti, and M. Selva, “Improving component substitution pansharpening through multivariate regression of MS+Pan data,” *IEEE trans. on Geoscience and remote sensing*, vol. 45, no. 10, pp. 3230–3239, October 2007.
 - [35] D. Fasbender, J. Radoux, and P. Bogaert, “Bayesian data fusion for adaptable image pansharpening,” *IEEE trans. on Geoscience and remote sensing*, vol. 46, no. 6, pp. 1847–1857, June 2008.
 - [36] Y. Gu, Y. Zhang, and J. Zhang, “Integration of spatial-spectral information for resolution enhancement in hyperspectral images,” *IEEE trans. on Geoscience and remote sensing*, vol. 46, no. 5, pp. 1347–1358, May 2008.
 - [37] A. Garzelli, F. Nencini, and L. Capobianco, “Optimal MMSE pansharpening of very high resolution multispectral images,” *IEEE trans. on Geoscience and remote sensing*, vol. 46, no. 1, pp. 228–236, January 2008.
 - [38] V. P. Shah, N. H. Younan, and R. L. King, “An efficient pan-sharpening method via a combined adaptive PCA approach and contourlets,” *IEEE trans. on Geoscience and remote sensing*, vol. 46, no. 5, pp. 1323–1335, May 2008.
 - [39] S. Pop, O. Lavielle, M. Donias, R. Terebes, M. Borda, S. Guillon, and N. Keskes, “A PDE based approach to three dimensional seismic data fusion,” *IEEE trans. on Geoscience and remote sensing*, vol. 46, no. 5, pp. 1385–1393, May 2008.
 - [40] P. M. Atkinson, E. Pardo-Igúzquiza, and M. Chica-Olmo, “Downscaling cokriging for super-resolution mapping of continua in remotely sensed images,” *IEEE trans. on Geoscience and remote sensing*, vol. 46, no. 2, pp. 573–580, February 2008.
 - [41] C. Thomas, T. Ranchin, L. Wald, and J. Chanussot, “Synthesis of multispectral images to high spatial resolution: A critical review of fusion methods based on remote sensing physics,” *IEEE trans. on Geoscience and remote sensing*, vol. 46, no. 5, pp. 1301–1312, May 2008.
 - [42] M. V. Joshi, S. Chaudhuri, and R. Panuganti, “A learning based method for image super-resolution using zoomed observations,” *IEEE Trans. on Systems, Man and Cybernetics, Part-B*, vol. 35, no. 3, pp. 527–537, June 2005.
 - [43] D. Capel and A. Zisserman, “Super-resolution from multiple views using learnt image models,” in *Proc. IEEE Int. Conf. on Computer Vision and Pattern Recognition*, 2001, vol. II, pp. 627–634.
 - [44] W. T. Freeman, T. R. Jones, and E. C. Pasztor, “Example-based Super-resolution,” *IEEE Computer Graphics and Applications*, vol. 22, no. 2, pp. 56–65, March/April 2002.
 - [45] M. V. Joshi, L. Bruzzone, and S. Chaudhuri, “A model based approach to multiresolution fusion in remotely sensed images,” *IEEE Trans. on Geoscience and Remote Sensing*, vol. 44, no. 9, pp. 2549–2562, September 2006.
 - [46] M. V. Joshi and A. Jalobeanu, “Multiresolution fusion in remotely sensed images using an IGMRF prior and MAP estimation,” in *IEEE Int. Geoscince and Remote Sensing Symposium*, Boston MA, USA, July, 2008, pp. 269–272.
 - [47] H. Aanaes, J. R. Sveinsson, A. A. Nielsen, T. Bøvith, and J. A. Benediktsson, “Model based satellite image fusion,” *IEEE trans. on Geoscience and remote sensing*, vol. 45, no. 5, pp. 1336–1346, May 2008.
 - [48] R. R. Schultz and R. L. Stevenson, “A Bayesian approach to image expansion for improved definition,” *IEEE Trans. on Image Processing*, vol. 3, no. 3, pp. 233–242, May 1994.
 - [49] A. N. Rajagopalan and S. Chaudhuri, “An MRF based approach to simultaneous recovery of depth and restoration from defocused images,” *IEEE Trans. on Pattern Analysis and Machine Intelligence*, vol. 21, no. 7, pp. 577–589, July 1999.
 - [50] D. Rajan and S. Chaudhuri, “Simultaneous estimation of super-resolved scene and depth map from low resolution defocused observations,” *IEEE Trans. on Pattern Analysis and Machine Intelligence*, vol. 25, no. 9, pp. 1102–1117, September 2003.
 - [51] P. Charbonnier, L. Blanc-Féraud, G. Aubert, and M. Barlaud, “Deterministic edge preserving regularization in computed imaging,” *IEEE Trans. on Image Processing*, vol. 6, pp. 298–311, Feb 1997.
 - [52] A. Jalobeanu, L. Blanc-Féraud, and J. Zerubia, “Hyperparameter estimation for satellite image restoration using a MCMC maximum likelihood method,” *Pattern Recognition*, vol. 35, no. 2, pp. 341–352, 2002.
 - [53] A. Jalobeanu, L. Blanc-Féraud, and J. Zerubia, “Adaptive parameter estim-

- tion for satellite image deconvolution,” Tech. Rep. 3956, INRIA Research Report, June 2000.
- [54] A. Jalobeanu, L. Blanc-Féraud, and J. Zerubia, “An adaptive Gaussian model for satellite image deblurring,” *IEEE Trans. on Image Processing*, vol. 13, no. 4, pp. 613–621, April 2004.
- [55] S. Geman and D. Geman, “Stochastic relaxation, gibbs distribution and the bayesian restoration of images,” *IEEE Trans. on Pattern Analysis and Machine Intelligence*, vol. 6, pp. 721–741, November 1984.
- [56] W. Cao, B. Li, and Y. Zhang, “A remote sensing image fusion method based on PCA transform and wavelet packet transform,” in *IEEE Int. Conf. Neural Networks and Signal Processing*, Nanjing, China, December, 2003, pp. 976–981.